

RESEARCH

Open Access



# AMD1, a cardiotoxicity target for Maduramicin

Zi-Feng Xie<sup>1,2</sup>, Han-Meng Liu<sup>2</sup>, Jia-Fan Zhao<sup>2</sup>, Yuan Gao<sup>1,2</sup>, Yuan-Long Zhao<sup>2</sup>, Jia-Yue Zheng<sup>3</sup>, Xiao-Wei Pei<sup>4</sup>, Ning Zhang<sup>5</sup> and Ge Tian<sup>6\*</sup>

## Abstract

**Objective** The aim of this study was to investigate AMD1 cardiotoxicity function for Maduramicin (Mad).

**Methods** SD rats were divided into control (Control) group and Mad treatment (3.5 mg/kg) group (Mad). After treatment with Mad for seven days, the levels of LDH and CK-MB in serum were detected, H&E staining and TUNEL staining were performed. In vitro, 1.0  $\mu$ m Mad was used for the subsequently experiment, observing cell apoptosis from Flow cytometry. Caspase-3 and AMD1 were detected in Western blotting. Flow cytometry and Western blotting were also performed after use of siRNA-AMD1-1. Then, analysis AMD1 potential function in cardiotoxicity from bioinformatics techniques including GO, KEGG, PPI, immune infiltration and molecular docking.

**Result** Maduramicin has myocardial toxic effects in vivo and vitro, which with AMD1 raised. When AMD1 was knocked down, toxic effects of Mad were alleviated. Apoptosis, proliferation and inflammation were the major pathophysiological changes in myocardial apoptosis process with AMD1-knockdown. This process involved in *IL1A*, *IL1B*, *PTGS2*, *VEGFA*, *VEGFC* and *HBEFG*, as hub genes related AMD1 cardiotoxicity function for Maduramicin. AMD1 was knocked down, their microenvironment changes: Effector memory CD4 T cell and Natural killer cell were more infiltrated, and Mast cell were less infiltrated.

**Conclusion** Mad exerted cardiotoxic effects by upregulating the AMD1 gene, which may be associated with cell apoptosis, proliferation and inflammatory response. AMD1 also had cardiotoxicity function, by the impact of both myocardial cells and the microenvironment they live.

**Keywords** Maduramicin, AMD1, Microenvironment

## Introduction

Maduramicin (Mad) was commonly added in feed additive for chickens and turkeys, which is a polyether ionophore antibiotic for preventing infection of coccidiosis [1]. It was proved its cardiotoxicity in many researches [2–5]. For clinical cases, Mad also could cause the cardiomyopathy with necrosis of heart [6]. Moreover, increasing cases on children who had taken poisoning food with Mad by accident have been reported led to rhabdomyolysis, renal failure and even death [7, 8]. Although the cases was limited, we should not ignore this condition. On the contract, it required more attention in case of the accident happened surrounding our work, which could cause

\*Correspondence:

Ge Tian

tiange810910@163.com

<sup>1</sup>Department of Anesthesiology, The First Affiliated Hospital of Jinzhou Medical University, Jinzhou, Liaoning 121000, China

<sup>2</sup>First Clinical Medical College, Jinzhou Medical University, Jinzhou, Liaoning 121000, China

<sup>3</sup>Stomatology Medical College, Jinzhou Medical University, Jinzhou, Liaoning 121000, China

<sup>4</sup>Department of Physical Medicine and Rehabilitation, Linghai Daling River Hospital, Linghai, Liaoning 121200, China

<sup>5</sup>Department of Hematology, The First Affiliated Hospital of Jinzhou Medical University, Jinzhou, Liaoning 121000, China

<sup>6</sup>Department of Cardiology, The First Affiliated Hospital of Jinzhou Medical University, Jinzhou, Liaoning 121000, China



© The Author(s) 2025. **Open Access** This article is licensed under a Creative Commons Attribution-NonCommercial-NoDerivatives 4.0 International License, which permits any non-commercial use, sharing, distribution and reproduction in any medium or format, as long as you give appropriate credit to the original author(s) and the source, provide a link to the Creative Commons licence, and indicate if you modified the licensed material. You do not have permission under this licence to share adapted material derived from this article or parts of it. The images or other third party material in this article are included in the article's Creative Commons licence, unless indicated otherwise in a credit line to the material. If material is not included in the article's Creative Commons licence and your intended use is not permitted by statutory regulation or exceeds the permitted use, you will need to obtain permission directly from the copyright holder. To view a copy of this licence, visit <http://creativecommons.org/licenses/by-nc-nd/4.0/>.

us medical workers have nothing but to look our poor patients lose their life.

S-adenosylmethionine decarboxylase proenzyme (AMD1) is involved in the synthesis process of spermine (SPM) and spermidine (SPD), as a key enzyme [9]. Polyamines have long been considered that it was associated with cellular processes and biochemical reaction. Not only did it include cell differentiation and proliferation, but also be conjugated to proteins and affect the protein function [10, 11]. Recent studies showed that embryonic stem cells (ESCs) self-renewal and maintain ESCs stemness were promoted by upregulating expression of multiple pluripotency factors, with the condition that AMD1 and its polyamine synthesis increased [12, 13]. Most studies considered that AMD1 is a potential target on oncogene research field, because it existed in multiple cancers and be paid attention to tumor therapy aspect [14–16]. However, research that AMD1 had function in cardiotoxicity field was extremely limited.

Actually, both SPM and SPD are small aliphatic cations mainly working as a mediator in the process of cell growth and differentiation, with multiple antioxidant, anti-inflammatory, and anti-apoptotic effects [17]. However, their changes in a recent research exposed the association with toxicometabolomics-based cardiotoxicity [18], which reveals limitation in the exploration. In present study, we first found that Maduramicin could upregulated expression of AMD1 in vivo and in vitro, which induced the myocardial cells apoptosis. Then investigated the role of AMD1 in cardiotoxicity by bioinformatics analysis.

## Materials and methods

### Chemical reagents

Absolute ethanol was obtained from Beijing Chemical Reagent Co. Maduramicin ammonium (CAS 84878-67-5; formula,  $C_{47}H_{80}O_{17}H_3N$ , Purity  $\geq 98\%$ ) was purchased from Shanghai TopScience Biotechnology Co. Maduramicin ammonium was diluted using DMEM (Hyclone; Cytiva) until the concentration of DMSO (Beijing Solarbio Science & Technology Co., Ltd.) was less than 0.1%.

### Cell culture and treatment

The H9c2 cells (cat. no. CL-0089; Purchased from Wuhan Pricella Biotechnology Co., Ltd.) were cultured in DMEM (Hyclone; Cytiva), supplemented with 10% FBS (Sera-Pro), penicillin G 100 U/mL and streptomycin 100 U/mL (Hyclone; Cytiva). The cells were incubated at 37 °C with 5% CO<sub>2</sub> in a humidified incubator. The state of the cells was monitored daily, and the fluid was changed according to the situation. Before the cells were washed twice with PBS, after which 3–5 mL of fresh complete medium was added to continue the culture. Subsequently, the fluid could be changed every two days based on the growth of

the cells, until the confluence reached 90%, and then cell passage was carried out at a ratio of 1:2 to 1:3. The cells used in the experiment were newly purchased cell lines in the laboratory (the company has tested them to be qualified), and cell passage was carried out according to the experimental requirements. The maduramicin-induced myocardial injury model was established as previously described. H9c2 cells were treated with different concentrations of maduramicin for 24 h. The morphology and number of cardiomyocytes were observed under light microscope.

### Animals and administration with mad

Thirty male SD rat, weighing 400–500 g, were purchased from the Laboratory Animal Center, China Medical University (Shenyang, China). The study was approved by the Ethical Committee at Jinzhou Medical University (NO:241063), and were in compliance with the guidelines set forth by the Guide for the Care and Use of Laboratory Animals. The rat were housed at room temperature (20–25 °C), relative humidity of 60%, subjected to a 12 h-light/dark cycle under conventional barrier protection, and supplied with water and feed ad libitum. After acclimatization to these conditions for 1 week, the rats were randomly divided into normal control (Control) group and Mad treatment group (Mad) (15 rat/group) by pairing comparison method. Before assigning the animals, they are first paired based on factors such as sex, age, weight, fetal differences, or other relevant criteria. Two essentially identical animals are grouped into pairs, and then each pair is randomly assigned to one of two groups, ensuring that the number of animals in both groups is equal. Furthermore, their fundamental characteristics—such as fetal differences, sex, age, and weight—are kept as similar as possible to minimize biological differences between the two groups of animals. A subacute Mad regimen (3.5 mg/kg), according to 1/10 LD50, was used. The rat in the Mad treatment group were intragastrically administered with Mad solution, which was dissolved in 2 ml of 100% ethanol and then diluted 10-fold with distilled water to obtain a final concentration of 0.2 mg/ml, and the control group received intragastric administration of water/vehicle daily for 7 d. At the end of the experiment, all animals were sacrificed by cervical dislocation, and heart tissues (retaining the ventricles only) were immediately removed and fixed in 4% paraformaldehyde or stored at –80 °C for further analysis.

### Cell viability assay

Cell viability was assessed using a CCK-8 assay (APEx-BIO Technology), after the treatment with different concentration of Mad (0, 0.25, 0.5, 1.0, 2.0  $\mu$ m), according to the manufacturer's protocol. A total of  $3 \times 10^3$  cells/well were cultured in 96-well plates and treated as described

above. Following treatment, 10  $\mu$ L CCK-8 solution was added to each well, and cells were further incubated for 1.5 h. The absorbance was measured at 450 nm using a microplate reader (Thermo Fisher Scientific).

#### **Lactate dehydrogenase and creatine kinase-myocardial band release assay**

When myocardial damage occurs, lactate dehydrogenase (LDH) and creatine kinase-myocardial band (CK-MB) are released into the culture medium. LDH and CK-MB activity were assessed using an LDH Assay Kit and CK-MB Assay Kit (Jiancheng Biotech Co., Ltd) according to the manufacturer's protocol.

#### **Hematoxylin and Eosin (H&E) staining**

Following the rinse with normal saline for three times, heart tissues were immersed in 4% paraformaldehyde for 24 h and embedded with conventional paraffin wax. 5- $\mu$ m-thick sections were obtained. Deparaffinization of the sections was performed and the sections were then stained with hematoxylin and eosin, prior to dehydration in a graded ethanol series and xylene. The sections were imaged with the aid of a light microscope (Nikon Eclipse E100).

#### **TUNEL staining**

TUNEL staining was performed according to the manufacturer's protocols of In Situ Cell Death Detection Kit<sup>®</sup> (Servicebio, Wuhan, China). For cardiac muscle of Mad-exposed rat, paraffin-embedded cardiac tissue sections were prepared, followed by TUNEL staining. Finally, photographs were taken under a fluorescence microscope (Nikon Eclipse C1, Japan) equipped with a digital camera. For quantitative analysis of the fluorescence intensity using TUNEL staining, the integral optical density (IOD) was measured by Image-Pro Plus 6.0 software (Media Cybernetics Inc., Newburyport, MA, USA).

#### **Cell transfection**

To knockdown AMD1, three specific short hairpin RNAs (siRNAs) targeting AMD1 (siRNA-AMD1-1 (AMD1-Rat-431, -CCCAAGAUCGAGUGGGGAUUAUCCACUCGGAUCUUGGGTT-), siRNA-AMD1-2 (AMD1-Rat-1020, -GGAAUGAAAUCGGAUGGAA TTUCCAUCGGAUUUCAUUCCTT-) or siRNA-AMD1-3 (AMD1-Rat-1255, -GCCAGAGCGCUAUGUUAATTUUGAACAUAGCGCUCUGGCTT-)), which regarded siRNA-NC as the negative control were designed and synthesized by GenePharma (Shanghai, China). Later, these vectors were transfected into cells with the application of Lipofectamine 2000 (Invitrogen, Shanghai GenePharma Co.,Ltd.). After 12 h of transfection, the transfection efficiency was evaluated by western

blotting. Choose the best one to finish the subsequent experiments.

#### **Detection of apoptosis by flow cytometry**

The apoptotic ratio of cardiomyocytes was detected by flow cytometry using an Annexin V- FITC apoptosis detection kit (Hangzhou MultiSciences Biotech Co.). The cardiomyocytes were harvested and washed twice with cold PBS, resuspended in binding buffer and incubated with 5  $\mu$ L Annexin V and 10  $\mu$ L PI at room temperature in the dark for 5 min. Flow cytometry was used to detect the apoptotic ratio of cells (FACSCalibur; BD Biosciences).

#### **Western blot analysis**

The cells were lysed in ice- cold RIPA lysis buffer to obtain total proteins. The protein concentration was detected using a BCA protein assay (Beyotime Institute of Biotechnology). Equal quantities of protein were loaded on an 8–12% SDS- gel, resolved using SDS- PAGE and transferred to a PVDF membrane. Subsequently, membranes were blocked with 5% (w/v) skimmed milk in TBS- T for 2 h at room temperature and incubated overnight with one of the following primary antibodies: Anti-cleaved-caspase 3 (1/1000, cat. no. 9661, Cell Signaling Technologies); Anti-AMD1 (1/1000, cat. no. 11052- 1- AP, ProteinTech Group); Anti-  $\beta$ -actin (1/2000, cat. no. GB11001, ServiceBio). The membranes were washed with TBS- T three times and incubated with a goat anti-rabbit IgG (H + L) HRP antibody (1:8000, Absin, cat. no. abs20040) for 1 h at room temperature. Protein bands were detected using a BeyoECL Plus Kit (Beyotime Institute of Biotechnology) according to the manufacturer's protocol. Relative densitometry analysis was performed using ImageJ version 1.52 (National Institutes of Health).

#### **Statistical analysis**

The results were shown as the mean  $\pm$  standard deviation (SD) in this study. Statistical analyses were carried out using t-test and one-way ANOVA followed by a Tukey's test. GraphPad Prism 9.5 software (La Jolla, USA) was used for statistical analysis.  $P < 0.05$  was considered to indicate statistical significance.

#### **Genes researching and intersection analysis**

GEO website (<https://www.ncbi.nlm.nih.gov/geo/>) was performed for researching GSE164881 and GSE151879 and GEO 2R analysis tool for differential genes in both two chips. Selection criteria ( $|\log_2 > 1|$  and  $p$ -value  $< 0.05$ ) were established to screen differentially expressed genes. GSE164881 included a microarray data of differentiated human keratinocytes treated with and without AMD1 inhibitor. We screened differentially expressed genes between the group of the control and the the

group of processing with AMD1 inhibitor. Genecards (<https://www.genecards.org/>) website was performed for researching related genes in myocardial cell apoptosis. Venn intersection analysis between GSE164881 and myocardial cell apoptosis was performed by Bioinformatics website (<https://www.bioinformatics.com.cn/>), for which these differentially expressed genes might be predicted as the changes of genes in the process of myocardial cell apoptosis after the AMD1 was regulated. GSE151879 described cardiomyocytes infected by SARS-CoV-2 recruit cardiotoxic macrophages, which showed the changing of the genes in immune cells with the abnormal condition. Their changes could be also a potential targets influencing the cardiomyocytes' microenvironment if Mad was absorbed. Thus, we chose it as a exploration for the changing of cardiomyocytes' microenvironment with AMD1 regulated.

#### GO and KEGG researching

The targets of intersection genes between GSE164881 and myocardial cell apoptosis were imported into David analysis website (<https://david.ncifcrf.gov/>) for the analysis of the Gene Ontology (GO) and Kyoto Encyclopedia of Genes and Genomes (KEGG). The results came from the bioinformatics website.

#### PPI analysis for hub genes

The targets of intersection genes between GSE164881 and myocardial cell apoptosis were imported into STRING database (<https://string-db.org/>), chose the Multiple proteins and Homo sapiens and get the PPI network. Then, adjusted that the minimum interaction threshold was 0.4 and hid individual targets with no changes for other parameters to get the protein interaction data file. Turned the file into the Cytoscape 3.9.1 software for the topology analysis and constructed the PPI network according to the Degree parameter. Cyto-Habba analysis tool for obtaining 20 Hub genes connection with their Degree parameter. Next, screened hub genes in GO and KEGG results.

#### Immune infiltration analysis

RStudio was performed for processing each sample's expression in GSE164881. RStudio's "single-sample GSEA (ssGSEA)" and "pheatmap" packages were used to estimate the difference of infiltration of 28 immune cell types using RStudio's "single-sample GSEA (ssGSEA)" and "pheatmap" packages for the intersection whole genes and hub genes between AMD1-knockdown group and myocardial injury. The scores of immune infiltration in each sample were statistically analyzed with the mean  $\pm$  standard deviation (SD) and one-way ANOVA followed by a Tukey's test in GraphPad Prism 9.5 software

(La Jolla, USA).  $P < 0.05$  was considered to indicate statistical significance.

#### Validation analysis

Differential analysis of hub genes in both GSE164881 and GSE151879. GSE164881 is the differential expression genes in whether AMD1 was knock-downed. GSE151879 is the differential expression genes in whether myocardial cell injury.

The protein structures and Mad 2D structures were downloaded from the Protein Data Bank (PDB) website and PubChem website. The Mad 2D structures were then converted to MOL2 format using OpenBabel software. Then, the length of hydrogen was calculated by molecular docking with AutoDock and PyMOL software.

## Result

#### Maduramicin has myocardial toxic effects in rats model

We divided SD rats into two groups: normal control (Control) group and maduramicin treatment (Mad) group. After treatment with Mad for seven days, the levels of lactate dehydrogenase (LDH) and creatine kinase-myocardial band (CK-MB) in serum were detected. As it shown in Fig. 1(a-b), those two substance in Mad group are much higher than NC ( $****p < 0.0001$ ). H&E staining in Fig. 1(c) has shown that more injury of myocardial tissue in maduramicin treatment than normal group. Besides, TUNEL staining was used to observe the cardiomyocyte apoptosis. In Fig. 1(d-e), The ratio of the apoptosis cells in Mad group is much higher than the control group. These findings supported that Maduramicin has myocardial toxic effects.

#### Maduramicin has cytotoxic effect on H9c2 cells with AMD1 upregulating

First, CCK-8 was performed for choosing the best Mad dose for the H9c2 cells from different concentration of Mad (0, 0.25, 0.5, 1.0, 2.0  $\mu\text{m}$ ). As shown in Fig. 2(a), we found that the vitality of the cells decreased with the increase of the Mad concentration. However, the survival rate of 1.0  $\mu\text{m}$  cells was between 50 and 60%. Therefore we considered 1.0  $\mu\text{m}$  was Mad's IC<sub>50</sub> to cardiomyocytes, which 1.0  $\mu\text{m}$  Mad was used for the subsequently experiment. Next, we separated H9c2 cells into two groups: maduramicin treatment (Mad) group and normal control (Control) group, which was treated without maduramicin. The morphology and number of cardiomyocytes under light microscope in Fig. 2(b) were observed that H9c2 cells treated with Mad had smaller quantity as well as more vacuolated changes than Control group. In Fig. 2(c), the smaller quantity with more cell death in Mad group can be observed from Flow cytometry. To explore the reason for apoptosis, we detected the expression on Caspase-3 and AMD1 in Western blotting. We

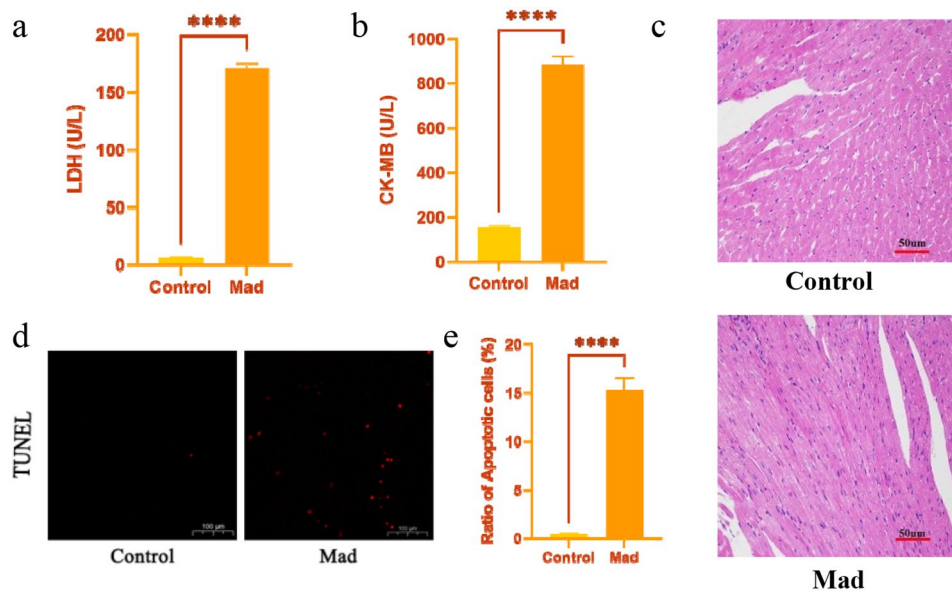


**Fig. 1** Maduramicin myocardial histopathological injury in rat. (a) The levels of LDH, and (b) CK-MB in serum were evaluated with commercial kits. \*\*\*\* $P < 0.0001$ . (c) The myocardial histopathological changes were measured by H&E staining (plotting scale: 50  $\mu\text{m}$ ). (d) Immunofluorescence reaction (plotting scale: 100  $\mu\text{m}$ ) and (e) ratio of cell apoptosis estimation was undertaken utilizing TUNEL. \*\*\*\* $P < 0.0001$

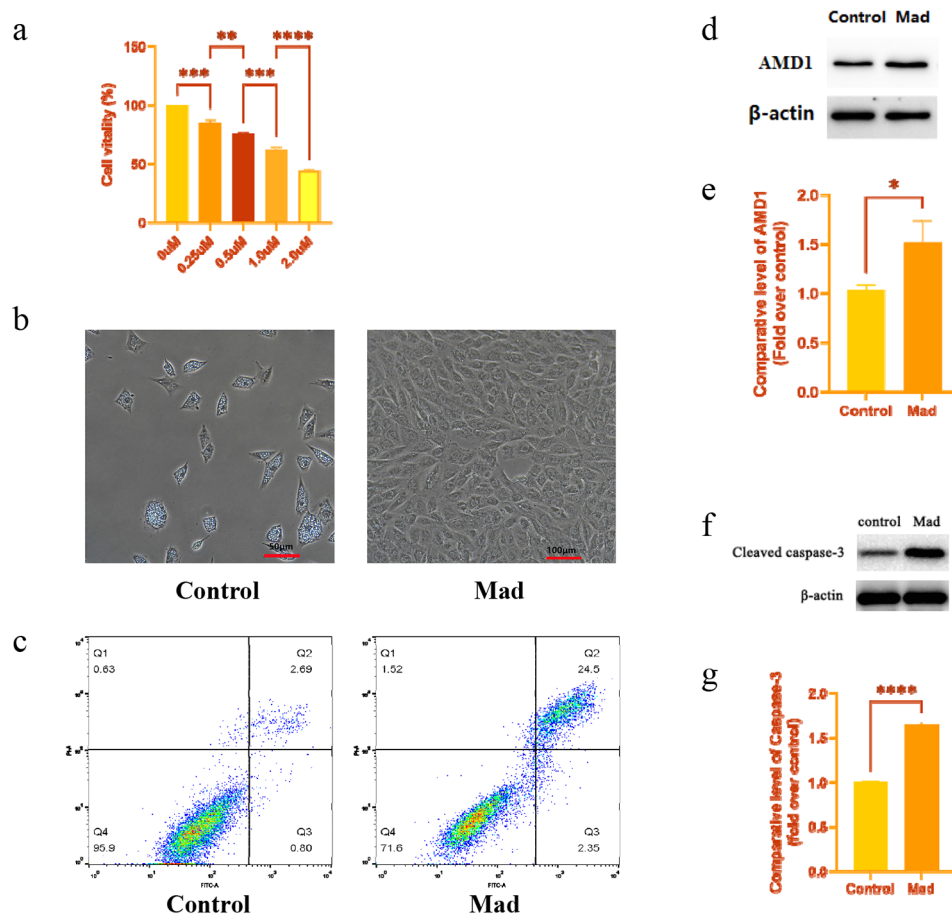


**Fig. 2** Maduramicin myocardial injury in H9c2 cells. (a) CCK-8 for the choice of the Mad's concentration. (b) Morphology and quantity of the H9c2 cells under the light microscope. Control: x100 (plotting scale: 50  $\mu\text{m}$ ), Mad: x200 (plotting scale: 100  $\mu\text{m}$ ) (c) Flow cytometry to observe H9c2 cell apoptosis. (d)&(e) The protein expression of AMD1 with Western blotting. \* $P < 0.05$ . (f)&(g) The protein expression of Caspase-3 with Western blotting. \*\*\*\* $P < 0.0001$

found that the protein expression of AMD1 (Fig. 2(d-e),  $*P < 0.05$ ) and Caspase-3 (Fig. 2(f-g),  $****P < 0.0001$ ) were upregulated. Our findings demonstrated that Maduramicin has myocardial cytotoxic effect and this had associated with AMD1 expression.

### The toxic effects of Maduramicin were alleviated after AMD1 knockdown

We chose three kinds of siRNA for knockdown AMD1. As shown in Fig. 3(a-b), siRNA-AMD1-1 is the best one for the subsequent experiment, which is much better than the other two siRNA with much lower AMD1 protein expression. In our finding in Flow cytometry, although the apoptosis increased in Mad treatment, cells death, with the use of siRNA-AMD1 after treatment with Mad is less than Mad treating only (Fig. 3(c)). Then we detected the AMD1 expression, as shown in Fig. 3(d-e), we found that Mad upregulated the expression of AMD1, though the volume of AMD1 was downregulated deliberately. However, it seems that Caspase-3 was regulated by AMD1, because we found that with siAMD1 was used for knockdown the expression of AMD1, the expression of caspase-3 was also be downregulated, as caspase-3 expression also be upregulated by treatment of Mad (Fig. 3(f-g)). These finding also expounded that AMD1

is a key factor in the apoptosis process of cardiomyocyte death induced by Maduramicin.

### Apoptosis, proliferation and inflammation can be predicted in treatment of AMD1-knockdown in myocardial apoptosis process by bioinformatics analysis

Chip(GSE164881) included the genes changes with the AMD1-knockdown. As shown in Fig. 4(a) and Fig. 4(c), 2050 differential genes in GSE164881 with the standard  $|\log_2 > 1|$  and  $p\text{-value} < 0.05$  were divided into upregulated genes and down regulated genes. 1322 upregulated genes and 981 down regulated genes were researched(Control vs. AMD1-Knockdown group). In Fig. 4(c), 4456 genes were able to be researched for myocardial apoptosis in Genecards databas. And, 506 intersection genes between GSE164881 and myocardial apoptosis (Fig. 4(b)). Therefore, the intersection genes of GSE164881 and myocardial apoptosis demonstrated treatment of AMD1-knockdown in myocardial apoptosis process.

For researching the changes of genes after the AMD1 was knocked-down in myocardial apoptosis process, GO and KEGG analysis of the intersection genes between GSE164881 and myocardial apoptosis were performed. Top 20 process was screened and the results were shown in Fig. 4(d-f). Figure 4(d) showed the biological process,

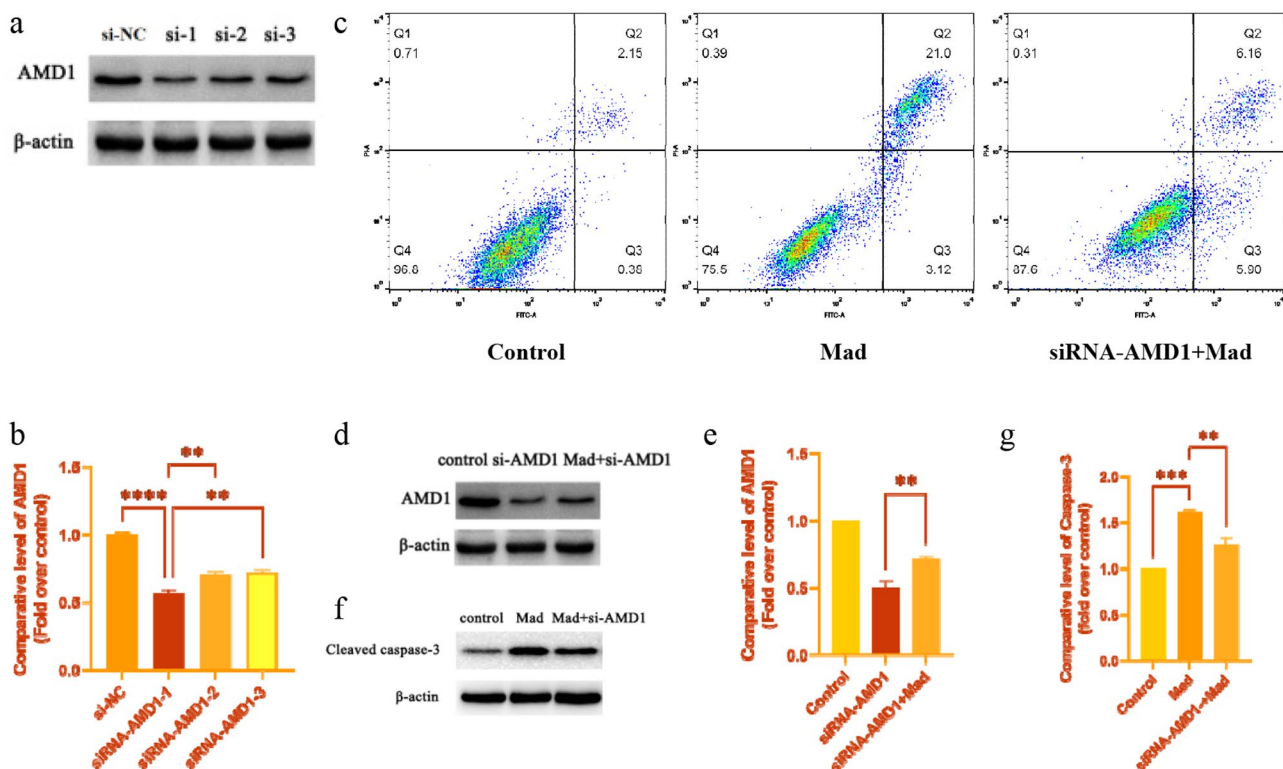


**Fig. 3** Maduramicin myocardial injury in H9c2 cells. (a)&(b) AMD1 protein expression with three kinds of siRNA-AMD1.  $***P < 0.001$ ,  $****P < 0.0001$ . (c) Flow cytometry to observe H9c2 cell apoptosis in control, Mad treatment and Mad treatment with siRNA-AMD1 transfection. (d)&(e) The protein expression of AMD1 with Western blotting.  $***P < 0.001$ ,  $****P < 0.0001$ . (f)&(g) The protein expression of Caspase-3 with Western blotting.  $***P < 0.001$

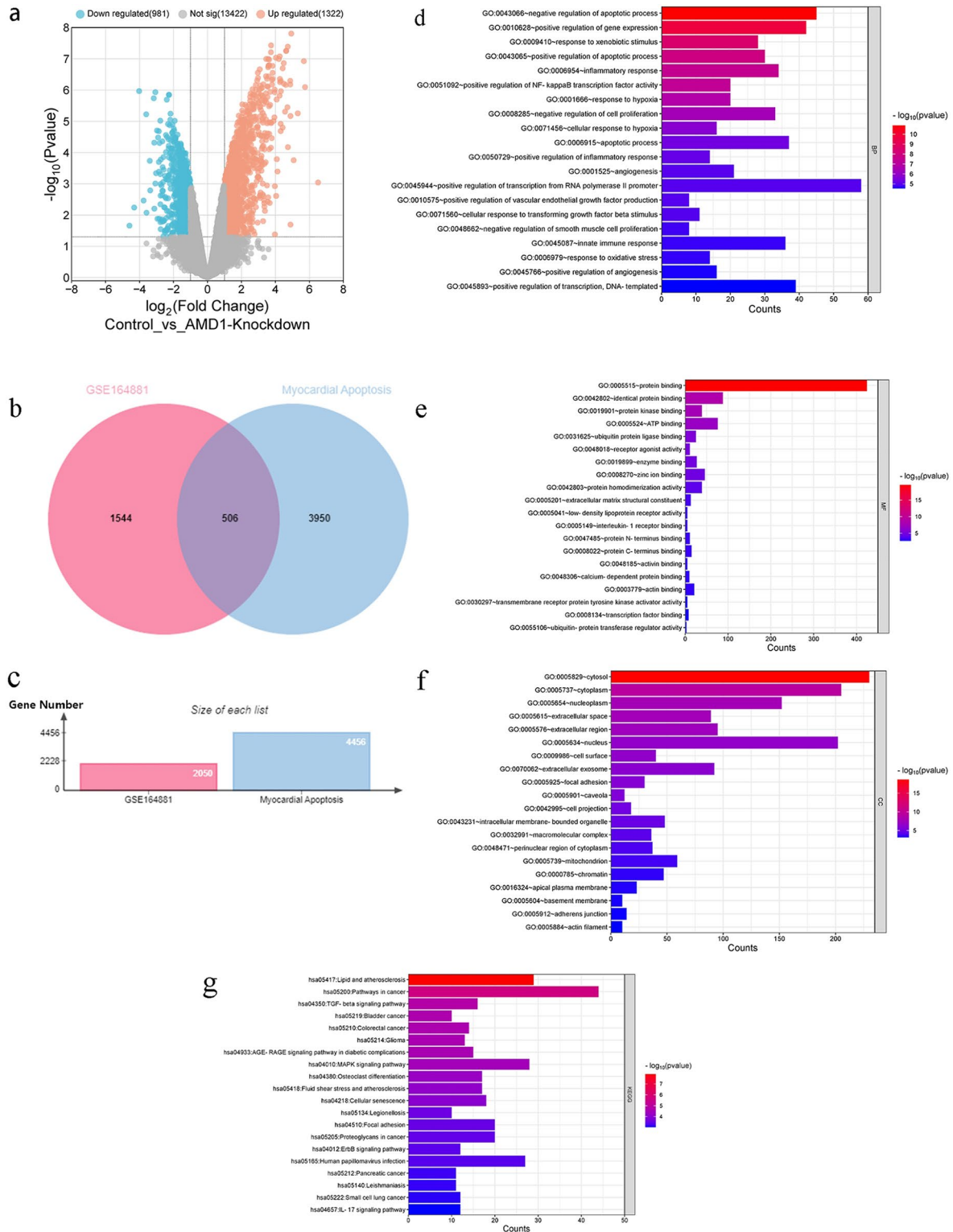


**Fig. 4** AMD1 and myocardial apoptosis bioinformatics analysis. **(a)** AMD1 related differential protein expression. **(b)** Venn diagram between AMD1 and myocardial apoptosis. **(c)** Genes quality of AMD1 and myocardial apoptosis. **(d)** GO biological process analysis. **(e)** GO molecular function analysis. **(f)** GO cellular component analysis. **(g)** KEGG analysis

which included (1) Apoptotic process: negative regulation of apoptotic process, positive regulation of apoptotic process and apoptotic process. (2) Cell proliferation: positive regulation of vascular endothelial growth factor production, negative regulation of cell proliferation, negative regulation of smooth muscle cell proliferation. (3) Inflammatory: inflammatory response, positive regulation of NF-kappaB transcription factor activity, positive regulation of inflammatory response, cellular response to transforming growth factor beta stimulus, and innate immune response. (4) Response to abnormal condition: response to xenobiotic stimulus, response to hypoxia and cellular response to hypoxia and response to oxidative stress. Figure 4(e) showed the molecular functions, which mainly included protein binding, interleukin-1 receptor binding and transcription factor binding etc. Figure 4(f) showed the cellular components, which mainly included cytosol and cytoplasm, nucleoplasm and nucleus, extra-cellular space and region, and cell surface. In KEGG analysis, as shown in Fig. 4(g) Lipid and atherosclerosis, Pathways in cancer, TGF-beta signaling pathway, MAPK

signaling pathway, Cellular senescence, Focal adhesion, Legionellosis, Human papillomavirus infection and IL-17 signaling pathway etc.

As summarized in the research of bioinformatics analysis, apoptosis, proliferation and inflammation were the major pathophysiological changes when AMD1 was knocked down in myocardial apoptosis process.

**Hub genes screening and their interaction between proteins**

To find out the interaction between proteins of AMD1-knockdown in myocardial apoptosis process, 506 genes intersection genes between GSE164881 and myocardial apoptosis, their space position was shown in Fig. 5(a) and Fig. 5(b), data from STRING and Cytoscape 3.9.1 separately. Then, to further explore the Hub genes, CytoHabba analysis tool was performed and 20 Hub genes with the top 20 Degree. Figure 5(c) and Fig. 5(d) showed the hub genes connection and their Degree value. In Fig. 5(c), the higher Degree value genes is, the deeper and bigger node genes have. In Fig. 5(D), Degree from 20 hub

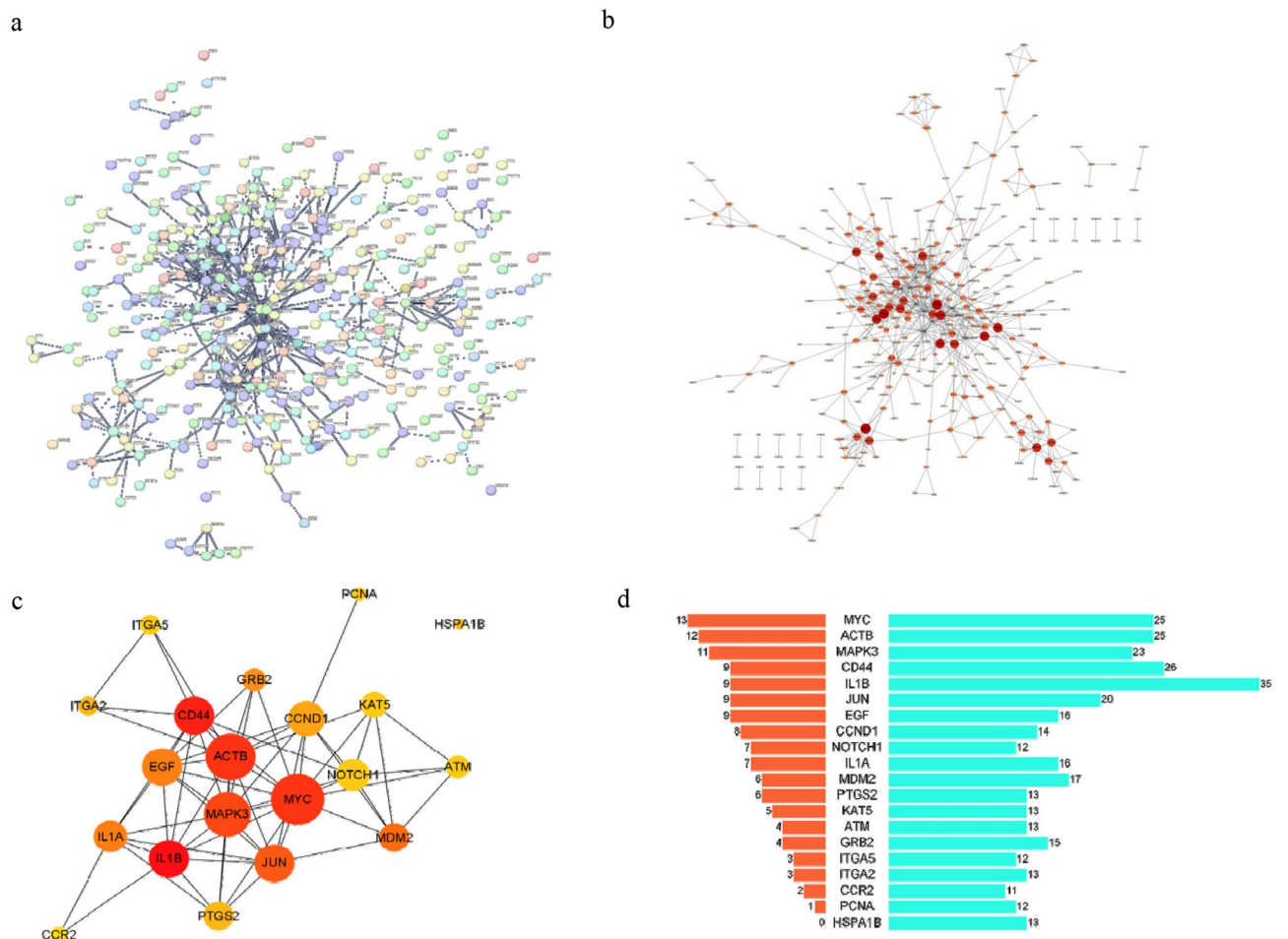


**Fig. 5** AMD1 and Myocardial Apoptosis in PPI analysis. (a) Diagram of STRING database analysis. (b) PPI Network from Cytoscape3.9.1 analysis. (c) 20 Hub genes from Cytohabba analysis. (d) Degree from 20 hub genes in Cytoscape (left in red) and Cytohabba (right in blue)

genes in Cytoscape (left in red) and Cytohabba (right in blue). As a result, 20 Hub genes with top Degree value were: *MYC*, *ACTB*, *MAPK3*, *CD44*, *IL1B*, *JUN*, *EGF*, *CCND1*, *NOTCH1*, *IL1A*, *MDM2*, *PTGS2*, *KAT5*, *ATM*, *GRB2*, *ITGA5*, *ITGA2*, *CCR2*, *PCNA*, *HSPA1B*. In addition, Hub genes in GO and KEGG analysis were also summarized in Supplementary Table 1.

#### Effector memory CD4 T cells, natural killer cell, and mast cell were the major immune infiltration cells

To find out the microenvironment of the myocardial apoptosis process, immune infiltration analysis was performed. Figure 6(a-d) showed differential immune infiltration analysis of total intersection genes between GSE164881 and cardiomyocyte apoptosis. Figure 6(a-b) is the general differential immune infiltration and it involved Effector memory CD8 T cell, Effector memory CD4 T cell, SIGLEC7, RPS9, Type 1 T helper cell, Type 2 T helper cell, Immature B cell, CD56 bright natural killer cell, KIR3DL1, Immature dendritic cell, TXNDC3, Mast cell and Neutrophil (\* $P < 0.05$ , \*\* $P < 0.01$ , \*\*\* $P < 0.001$ , \*\*\*\* $P < 0.0001$ ). Next, after the immune cells were classified, differential immune infiltration included Central memory CD8 T cell, Effector memory CD8 T cell, Central memory CD4 T cell, Effector memory CD4 T cell, Type 1 T helper cell, CD56bright natural killer cell, Type 2 T helper cell, Immature dendritic cell, SIGLEC7, Gamma delta T cell, RPS9, Memory B cell, Row 20, KIR3DL1, TXNDC3, Mast cell (Fig. 6(c-d), \* $P < 0.05$ , \*\* $P < 0.01$ ).

To further explore the relationship between Hub genes of the myocardial apoptosis process and the microenvironment the cells living, immune infiltration analysis of 20 Hub genes from PPI was performed. Effector memory CD4 T cell, Natural killer cell and Mast cell were enriched (Fig. 6(e-f), \*\*\*\* $P < 0.0001$ ). To summary, with AMD1 was knocked down, Effector memory CD4 T cell and Natural killer cell were more infiltrated, and Mast cell were less infiltrated.

#### Differential validation analysis

To validate the cardiotoxic reactions when the genes changes, 20 Hub genes were found in GSE164881(chips of AMD1-Knockdown) and GSE151879(chips of cardiotoxic reactions). *IL1A*, *IL1B*, *PTGS2*, *VEGFA*, *VEGFC* and *HBEFG* were upregulated in GSE164881 and downregulated in GSE151879, which demonstrated that when AMD1 was higher, these genes expression were decreased and might cause the cardiotoxic reactions (Fig. 7(a-b)).

To validate whether the genes with the cardiotoxic reactions were produced by Mad, molecular docking was performed. Binding ability was calculated according to the affinity score. Affinity  $< -7$  kcal/mol represents

stronger binding activity,  $-4$  to  $-7$  kcal/mol means moderate activity, and affinity  $> -4$  kcal/mol suggests weak binding activity [19]. It was found that *AMD1* ( $-11.85$ ), *IL1B* ( $-9.17$ ), *PTGS2* ( $-12.07$ ), and *VEGFA* ( $-8.52$ ) exhibited stronger binding activity with Mad, while *IL1A* ( $-6.56$ ), *VEGFC* ( $-6.06$ ) and *HBEFG* ( $-6.44$ ) showed moderate binding activity with it. Besides, the associations of *AMD1*, *IL1A*, *IL1B*, *PTGS2*, *VEGFA*, *VEGFC* and *HBEFG* with Mad were separately shown using PyMOL software. Molecular docking results were shown in Fig. 7(c-i). Mad was painted in wheat and genes were painted in orange. The hydrogen bonds were represented as yellow dotted lines in the diagrams. The quantity and length of hydrogen bonds and amino acids names with their position in the amino acid sequence were summarized in Table 1.

#### Discussion

In this present study, We first found that Maduramicin has myocardial toxic effects in vivo and vitro. After the upregulated Caspase-3 was detected, we further believed that Mad has cardiotoxic function via apoptosis pathway. Many researches were also proved Mad's cardiotoxicity which might be associated with apoptosis pathway [2–5]. Therefore, it is undoubted to consider Mad, as a cardiotoxic function poison, inducing apoptosis pathway in myocardial cells. We have previously studied drugs associated with cardiotoxicity, such as doxorubicin and alcohol, which exhibit apoptotic effects similar to those of Mad. All of them induced apoptosis in cardiomyocytes. Although Mad is less commonly observed than doxorubicin and alcohol, it is also cardiotoxic and holds significant value for toxicological research [20–23].

AMD1 might be a potential target for Mad's cardiotoxicity. After Mad was added into myocardial cells, the expression of AMD1 was improved. We considered that AMD1 might be involved in the process of Mad's myocardial toxic effects. As we mentioned in the introduction, toxicometabolomics-based cardiotoxicity was observed with elevated levels of polyamines, spermine and spermidine, noted in a recent report, and they considered it have been linked through numerous in vivo models with cardiac hypertrophy [18]. AMD1, as a key involved in the synthesis process of spermine and spermidine. This result as similar as ours, which exposed AMD1 cardiotoxicity changing in the myocardial cells. For further exploring whether AMD1 was a key role in cardiotoxic process, we used siRNA-AMD1 to disturb the expression of AMD1. We found that with the addition of siRNA-AMD1, AMD1 was downregulated. Subsequently, Mad cardiotoxic effect was also be decreased. This phenomenon demonstrated that AMD1 played an important role in cardiotoxicity. The translational of AMD1 impacted cell differentiation and proliferation via regulating the volume of polyamines. In some researches,

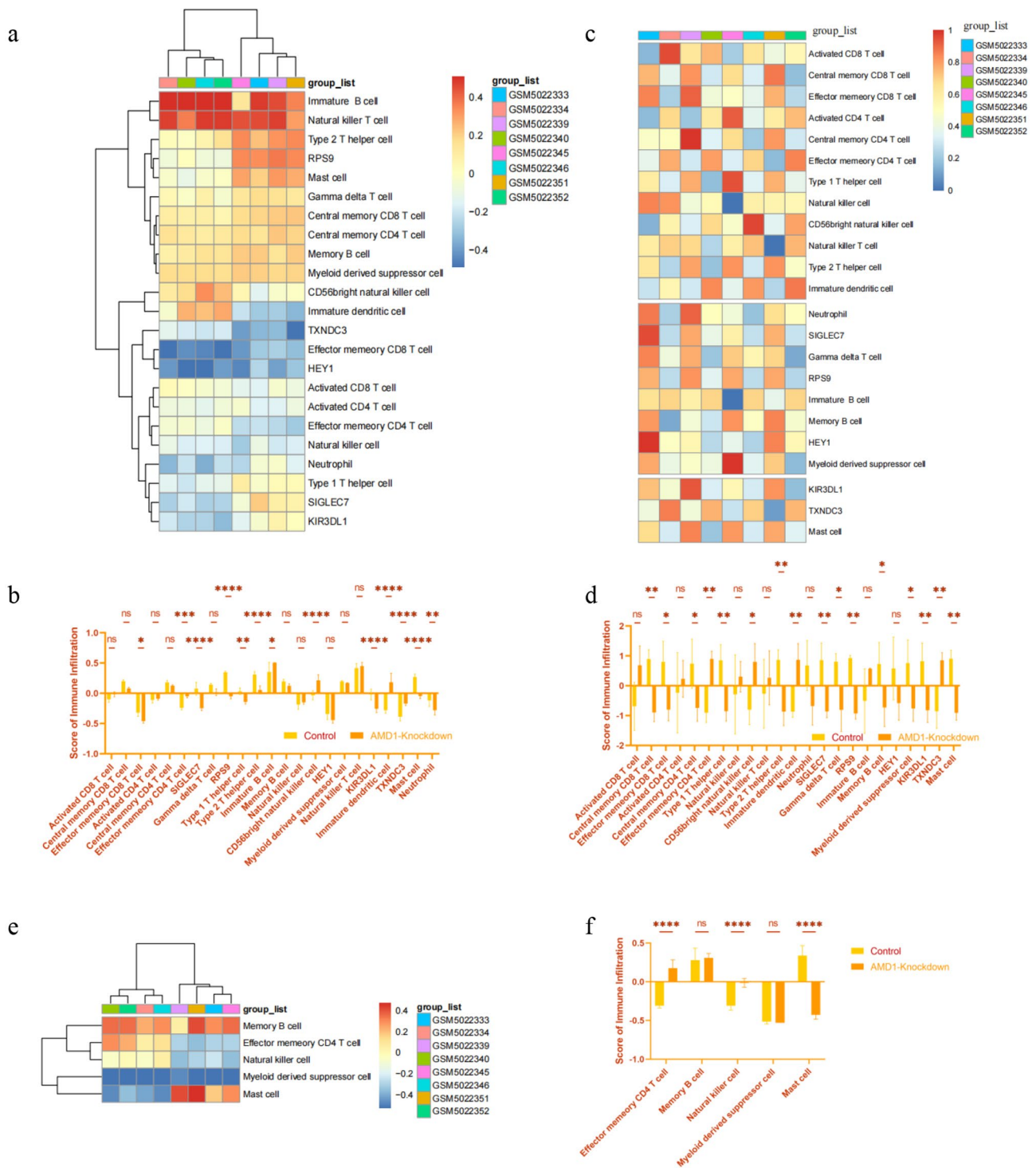


**Fig. 6** ssGSEA immune infiltration analysis. **(a-b)** General Differential immune infiltration analysis of total intersection genes between GSE164881 and cardiomyocyte apoptosis. **(c-d)** Classified differential immune infiltration analysis of total intersection genes between GSE164881 and cardiomyocyte apoptosis. **(e-f)** Differential immune infiltration analysis of Hub genes between GSE164881 and cardiomyocyte apoptosis. \* $P < 0.05$ , \*\* $P < 0.01$ , \*\*\* $P < 0.001$ , \*\*\*\* $P < 0.0001$

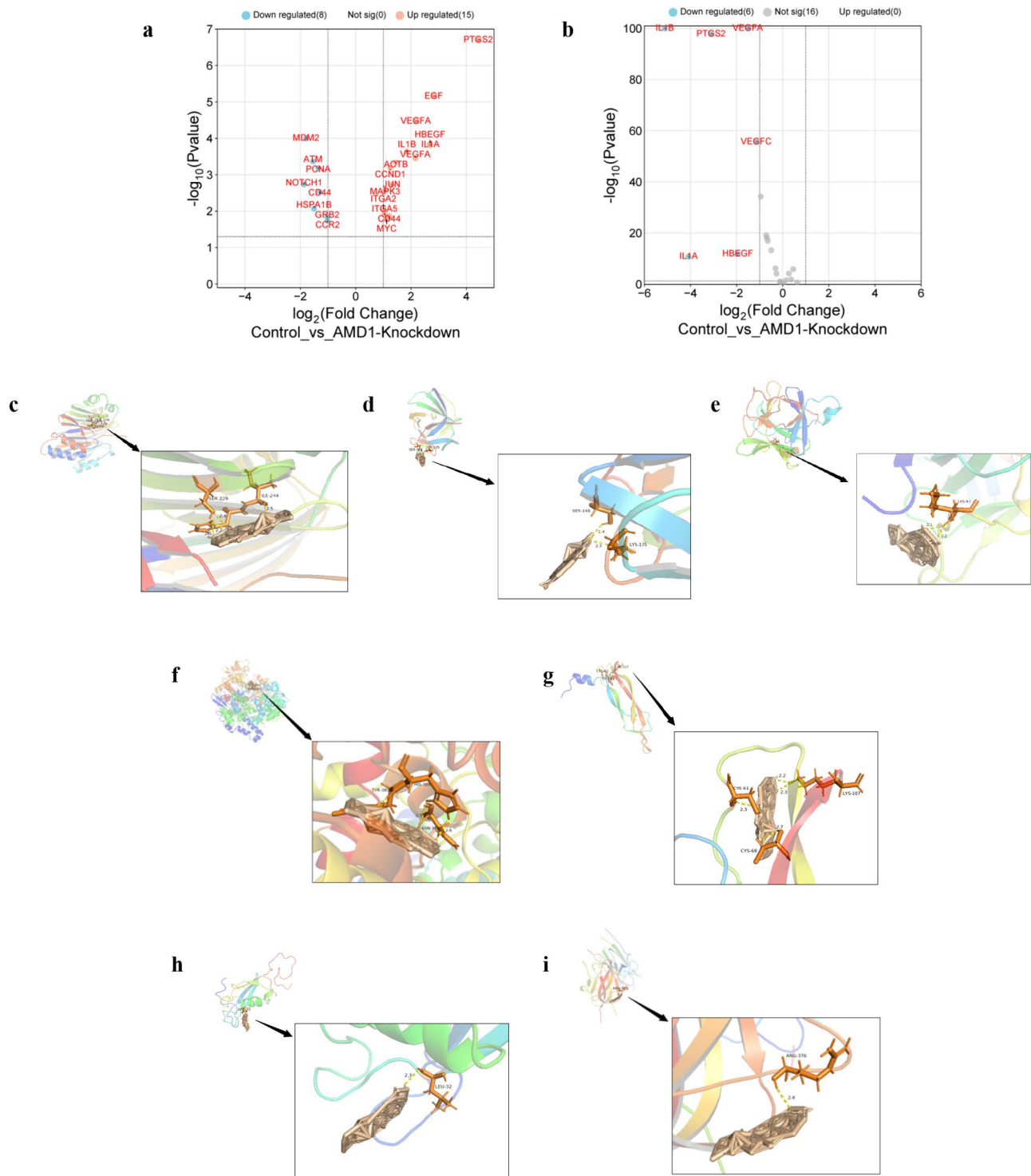


**Fig. 7** Differential validation analysis. **(a)** Differential hub genes for Cardiotoxic reactions in GSE164881. **(b)** Differential validation genes for Cardiotoxic reactions in GSE151879. **(c-i)** Molecular docking between Mad and AMD1 **(c)**, IL1A **(d)**, IL1B **(e)**, PTGS2 **(f)**, VEGFA **(g)**, VEGFC **(h)** and HBEGF **(i)**

elevated expression of AMD1 was correlated with abnormal state in body, such as the tumor's growth [14, 24]. In clinical, it was obvious that patients who had higher AMD1 expression, poor survival and prognosis they had [24]. The similar result with us, with the AMD1 enhanced

in cells, increasingly tendency of cells apoptosis was more easily to happen. Our result showed toxic effect function in normal cells was improved with AMD1 up-regulated in myocardial cell. However, when AMD1 inhibitors were co-administered with Mad, cells apoptosis was mediated.

**Table 1** Molecular docking between genes and mad

Genes docking with Mad	Quantity (with length(Å)) of hydrogen bonds	Amino acids names (their position in sequence)
AMD1	4 (2.2, 2.4, 2.5, 2.5)	SER(229), ILE(244)
IL1A	2 (2.3, 2.4)	LYS(135), SER(148)
IL1B	2 (2.1, 2.1)	LYS(93)
PTGS2	3 (2.2, 2.6, 2.9)	ASN(382), TYR(385), HIS(386)
VEGFA	4 (2.2, 2.3, 2.3, 2.7)	CYS(61), CYS(68), LYS(107)
VEGFC	1 (2.4)	ARG(376)
HBEFG	1 (2.3)	LEU(32)

Abbreviation: SER: Serine, ILE: Isoleucine, LYS: Lysine, ASN: Asparagine, TYR: Tyrosine, HIS: Histidine, CYS: Cysteine, ARG: Arginine, LEU: Leucine

This demonstrated that AMD1 inhibitors could mitigate cardiotoxicity. According to the information above, we inferred that AMD1 might not be the normal formation in cellular biological process. If the expression of AMD1 was enhanced, toxic reaction could also be increased. A recent research shows that high level radon exposure could enhance the risk of lung cancer, with the expression of AMD1 increased [25]. This research helped us proved our deduction further.

However, how could the AMD1 impact our body, especially in the myocardial tissue? We performed bioinformatics analysis in AMD1 function. In the GO and KEGG pathways analysis, we enriched the major process included (1) Apoptotic and cell proliferation process (Response based on the cell itself). (2) Inflammatory and response to abnormal condition (Response in the microenvironment the cells living in). In the Hub genes screening, we summarized the correlation between the hub genes and results in GO and KEGG pathways enrichment. For apoptotic process, it is included *MAPK3*, *IL1B*, *IL1A* and *PTGS2* etc. For proliferation process, *IL1B*, *IL1A*, *PTGS2* etc. Besides, MAPK signaling pathway and TGF-beta signaling pathway were also be mentioned and *MAPK3* was enriched. These findings also help us prove our opinion that with the changes of *MAPK3*, fate of the cell might be changed. However, *IL1B*, *EGF* and *IL1A* were at the position of extracellular space and region, which demonstrated that it had connection with the microenvironment cell living in. For Inflammatory response, innate immune response and IL-17 signaling pathway were involved. *IL1B*, *IL1A* and *PTGS2* were enriched. Moreover, *PTGS2* also involved the response to xenobiotic stimulus and oxidative stress, and pathway of Human papillomavirus infection. In addition, we also found that Effector memory CD4 T cell and Natural killer cell were more infiltrated, and Mast cell were less infiltrated from our immune infiltrated analysis. In some researches, there are plenty of findings supporting our opinion. Hu had enriched the *MAPK3* in apoptotic

process [26]. Gunel had found that *MAPK3* was down-regulated with higher apoptosis in vitro experiment [27]. Another research showed that cardiomyocyte apoptosis was induced by downregulating *MAPK3* [28]. These researches tells us with the *MAPK3* function in proliferation and apoptosis process. *IL1A* is constitutively present in keratinocytes and epithelial cells, however some cells like macrophages, endothelial cells, fibroblasts express the *IL1A* precursor only upon activation [29]. It was considered as “a loaded gun”, because it can change the microenvironment changes by releasing a proinflammatory alarmin when cell necrosis happening, to alert tissues surrounding and cause local tissue inflammation [30]. Although some researchers thought *IL1B* secretion is largely restricted to circulating monocytes and had connection with the systemic inflammation, some CD4 T cell subsets express higher levels of pro*IL1B* than unstimulated monocytes [29, 31]. In Netea’s research, *IL1B* was found its function in regulating T cell polarization and had correlation with the inflammation [31]. *PTGS2* also has connection with apoptosis and inflammation. In cardiovascular research, *PTGS2*, a protein related with ferroptosis and pyroptosis, was considered as a hub gene in human coronary artery atherosclerosis [32]. It also played an important role in pathologies associated with inflammatory signaling [33]. Actually, *PTGS2*, commonly known as cyclooxygenase-2 (*COX-2*), expressed at very low levels under physiological conditions [34–36]. However, its expression and activation can be induced by pro-inflammatory cytokines and growth factors, which activated inflammation-related pathways [37]. Similar with our findings, we also found *IL1A*, *IL1B* and *PTGS2* were substance deeply impacted the cells process via changing the microenvironment and causing the inflammation. Hub genes in our list were verified in myocardial apoptosis chips and molecular docking with Mad. *IL1A*, *IL1B* and *PTGS2* were upregulated in GSE164881 and downregulated in GSE151879, which demonstrated that when AMD1 was higher, these genes expression were decreased and might cause the cardiotoxic reactions. From this result, we inferred that, if Mad enhanced the expression of AMD1, the expression of *IL1A*, *IL1B* and *PTGS2* were impacted, which might induced the injury of myocardial tissue. These findings showed AMD1 impact our body by myocardial cell itself and the microenvironment it lives in.

Our study has some limitations:1. First, we found that the cardiotoxic effects of Mad were reflected by the abnormal increase of AMD1 expression. However, the cardiotoxic effects and harms of Mad may be different in animals and humans due to differences in species, or differences in dose and compensation mechanisms. 2. Second, our analysis method is based on bioinformatics and does not directly analyze the genetic changes

of cardiomyocytes through single-cell sequencing, and the genome chip may differ from real cardiomyocytes. Hence, the predicted genetic changes may be limited. However, these limitations are not enough to obscure the significance of the study in this paper, which still provides a theoretical support for the increase of myocardial toxicity by Mad and points out that the AMD1 inhibitors may serve as a potential antidote to reduce Mad-induced cardiotoxicity.

## Conclusion

Mad exerted cardiotoxic effects by upregulating the AMD1 gene. AMD1 had cardiotoxicity functions, by the impact of both myocardial cells themselves and the microenvironment they live, which was associated with cell apoptosis, proliferation and inflammatory response. Our findings showed that Mad as a poison for myocardial cells by AMD1, which highlighted the AMD1 function in cardiotoxic effects, broaden the cognition of AMD1-treated drugs for the multi clinical appliance.

## Supplementary Information

The online version contains supplementary material available at <https://doi.org/10.1186/s40360-025-00897-0>.

Supplementary Material 1

Supplementary Material 2

## Acknowledgements

We would like to express our gratitude to all individuals who contributed to the execution of this study. For me, as the first author of the article, have the opportunity to conceive and write the paper. Therefore, I am immensely grateful to my mentor, GT, and all the members of our team. I am a medical undergraduate, so this article is closely related to my mentor's careful instruction. She is my main mentor for scientific research. She gave me a lot of encouragement when I felt frustrated. She gave me the opportunity to complete the work freely and write the whole article. Although the process of scientific research is full of difficulties and hardships, I find happiness and enjoyment in it. Also, I am grateful to all the reviewers for their feedback on the article; you have also been my mentors. All the advice you mentioned inspires me to improve the article and enhance our experience. At last, thank you to all the people who supported me.

## Author contributions

GT and ZF-X conceived major introduction. GT offered the data in vivo and vitro and checking. ZF-X made the bioinformatics analysis and wrote the manuscript. HM-L performed the immune analysis. Molecular docking was completed by YL-Z. YG summarized the articles. Others had given advice in the revision of the article in thought and direction for revising. All authors contributed to the research and approved the final manuscript for publication.

## Funding

This work was supported financially by College Students Innovation and Entrepreneurship Training Program (X202410160073 to Zi-Feng Xie, Han-Meng Liu and Ge Tian) and Liaoning Province Science and Technology Plan Joint Plan Natural Science Fund project (2024-MSLH-137 to Ge Tian).

## Data availability

No datasets were generated or analysed during the current study.

## Declarations

### Ethics approval and consent to participate

The animals in vivo experiment has been approved by Ethics Committee of the Laboratory Animal Center in Jinzhou Medical University (NO:241063).

### Consent for publication

We, all the author, allowed to publish the article.

### Competing interests

The authors declare no competing interests.

Received: 2 August 2024 / Accepted: 7 March 2025

Published online: 11 March 2025

## References

1. Dorne JL, et al. Risk assessment of coccidiostats during feed cross-contamination: animal and human health aspects. *Toxicol Appl Pharmacol*. 2013;270(3):196–208.
2. Chen X, et al. Maduramicin induces cardiac muscle cell death by the ROS-dependent PTEN/Akt-Erk1/2 signaling pathway. *J Cell Physiol*. 2019;234(7):10964–76.
3. Gao X, et al. Transcriptome profile analysis reveals cardiotoxicity of Maduramicin in primary chicken myocardial cells. *Arch Toxicol*. 2018;92(3):1267–81.
4. Gao X, et al. Maduramicin triggers methuosis-like cell death in primary chicken myocardial cells. *Toxicol Lett*. 2020;333:105–14.
5. Chen X, et al. Maduramicin induces apoptosis and necrosis, and blocks autophagic flux in myocardial H9c2 cells. *J Appl Toxicol*. 2018;38(3):366–75.
6. Fourie N, et al. Cardiomyopathy of ruminants induced by the litter of poultry fed on rations containing the ionophore antibiotic, Maduramicin. I. Epidemiology, clinical signs and clinical pathology. *Onderstepoort J Vet Res*. 1991;58(4):291–6.
7. Jayashree M, Singhi S. Changing trends and predictors of outcome in patients with acute poisoning admitted to the intensive care. *J Trop Pediatr*. 2011;57(5):340–6.
8. Sharma N, et al. Toxicity of Maduramicin. *Emerg Med J*. 2005;22(12):880–2.
9. Pegg AE. S-Adenosylmethionine decarboxylase. *Essays Biochem*. 2009;46:25–45.
10. Pegg AE. Mammalian polyamine metabolism and function. *IUBMB Life*. 2009;61(9):880–94.
11. Yu CH, et al. Uncovering protein polyamination by the spermine-specific antiserum and mass spectrometric analysis. *Amino Acids*. 2015;47(3):469–81.
12. Zhang D, et al. AMD1 is essential for ESC self-renewal and is translationally down-regulated on differentiation to neural precursor cells. *Genes Dev*. 2012;26(5):461–73.
13. Zhao T, et al. A role for polyamine regulators in ESC self-renewal. *Cell Cycle*. 2012;11(24):4517–23.
14. Zabala-Letona A, et al. mTORC1-dependent AMD1 regulation sustains polyamine metabolism in prostate cancer. *Nature*. 2017;547(7661):109–13.
15. Evageliou NF, et al. Polyamine antagonist therapies inhibit neuroblastoma initiation and progression. *Clin Cancer Res*. 2016;22(17):4391–404.
16. Ali HEA, et al. Dysregulated gene expression predicts tumor aggressiveness in African-American prostate cancer patients. *Sci Rep*. 2018;8(1):16335.
17. Galasso L, et al. Polyamines and physical activity in musculoskeletal diseases: A potential therapeutic challenge. *Int J Mol Sci*. 2023; 24(12).
18. Al Sultan A, Rattray Z, Rattray NJW. Toxicometabolomics-based cardiotoxicity evaluation of Thiazolidinedione exposure in human-derived cardiomyocytes. *Metabolomics*. 2024;20(2):24.
19. Cui Q, et al. A network Pharmacology approach to investigate the mechanism of Shuxuening injection in the treatment of ischemic stroke. *J Ethnopharmacol*. 2020;257:112891.
20. Tian G, et al. FGF12 restrains mitochondria-dependent ferroptosis in doxorubicin-induced cardiomyocytes through the activation of FGFR1/AMPK/NRF2 signaling. *Drug Dev Res*. 2024;85(1):e22149.
21. Tian G, Li J, Zhou L. Ginsenoside Rg1 regulates autophagy and endoplasmic reticulum stress via the AMPK/mTOR and PERK/ATF4/CHOP pathways to alleviate alcohol-induced myocardial injury. *Int J Mol Med*. 2023; 52(1).
22. Zhou L, Zhai G, Tian G. CRIF1 attenuates doxorubicin-mediated mitochondrial dysfunction and myocardial senescence via regulating PDXN. *Aging*. 2024;16(6):5567–80.

23. Tian G, et al. Empagliflozin alleviates ethanol-induced cardiomyocyte injury through Inhibition of mitochondrial apoptosis via a SIRT1/PTEN/Akt pathway. *Clin Exp Pharmacol Physiol*. 2021;48(6):837–45.
24. Liao R, et al. AMD1 promotes breast cancer aggressiveness via a spermidine-*elf5A* hypusination-TCF4 axis. *Breast Cancer Res*. 2024;26(1):70.
25. Zhang P, et al. Alteration of genome-wide DNA methylation in non-uranium miners induced by high level radon exposure. *Mutat Res Genet Toxicol Environ Mutagen*. 2023;891:503683.
26. Hu W, Chen X. Identification of hub ferroptosis-related genes and immune infiltration in lupus nephritis using bioinformatics. *Sci Rep*. 2022;12(1):18826.
27. Gunel NS, et al. Investigation of cytotoxic and apoptotic effects of disodium pentaborate decahydrate on ovarian cancer cells and assessment of gene profiling. *Med Oncol*. 2022;40(1):8.
28. Liu Y, et al. MicroRNA-15b deteriorates hypoxia/reoxygenation-induced cardiomyocyte apoptosis by downregulating Bcl-2 and MAPK3. *J Investig Med*. 2018;66(1):39–45.
29. Netea MG, et al. Inflammasome-independent regulation of IL-1-family cytokines. *Annu Rev Immunol*. 2015;33:49–77.
30. Anders HJ. Of inflammasomes and alarmins: IL-1 $\beta$  and IL-1 $\alpha$  in kidney disease. *J Am Soc Nephrol*. 2016;27(9):2564–75.
31. Pulugulla SH, et al. Distinct mechanisms regulate IL1B gene transcription in lymphoid CD4 T cells and monocytes. *Cytokine*. 2018;111:373–81.
32. Zhou Y, et al. Verification of ferroptosis and pyroptosis and identification of PTGS2 as the hub gene in human coronary artery atherosclerosis. *Free Radic Biol Med*. 2021;171:55–68.
33. Martín-Vázquez E, et al. The PTGS2/COX2-PGE(2) signaling cascade in inflammation: pro or anti? A case study with type 1 diabetes mellitus. *Int J Biol Sci*. 2023;19(13):4157–65.
34. Kraemer SA, Meade EA, DeWitt DL. Prostaglandin endoperoxide synthase gene structure: identification of the transcriptional start site and 5'-flanking regulatory sequences. *Arch Biochem Biophys*. 1992;293(2):391–400.
35. Dubois RN, et al. Cyclooxygenase in biology and disease. *Faseb J*. 1998;12(12):1063–73.
36. Alexanian A, Sorokin A. Cyclooxygenase 2: protein-protein interactions and posttranslational modifications. *Physiol Genomics*. 2017;49(11):667–81.
37. Klein T, et al. Regulation of cyclooxygenase-2 expression by Cyclic AMP. *Biochim Biophys Acta*. 2007;1773(11):1605–18.

### Publisher's note

Springer Nature remains neutral with regard to jurisdictional claims in published maps and institutional affiliations.